

## A new technique for combined dynamic compression-shear test

*P.D. Zhao<sup>1\*</sup>, F.Y. Lu<sup>1</sup>, R. Chen<sup>1</sup>, G.L. Sun<sup>2,3</sup>, Y.L. Lin<sup>1</sup>, J.L. Li<sup>1</sup>, L. Lu<sup>4</sup>*

1. College of Science, National Univ. of Defense Technology, 410073 Changsha, China
2. College of Optoelectronics Science and Engineering, National Univ. of Defense Technology, 410073 Changsha, China
3. Institute of systems and mathematics, Naval Aeronautical Engineering Institute, 264001 Yantai, China
4. College of electronic science and engineering, National Univ. of Defense Technology, 410073 Changsha, China

\*Corresponding author: [Zhaopengduo@163.com](mailto:Zhaopengduo@163.com)

**Abstract:** We propose a dynamic combined compressive and shear experimental technique at high strain rates ( $10^2$ - $10^4$  s<sup>-1</sup>). The main apparatus is mainly composed of a projectile, an incident bar and two transmitter bars. The close-to-specimen end of the incident is wedge-shaped with 90 degree. In each experiment, there are two identical specimens respectively agglutinated between one side of the wedge and one of transmitter bars. When a loading impulse travels to specimens along the incident bar, because of the special geometrical shape, the interface of specimen glued with the incident bar has an axial and a transverse velocity. Thus, the specimens endure the combined pressure-shear loading at high strain rates. The compression stress and strain are obtained by strain gages located on the bars; the shear stress is measured by two piezoelectric crystals of quartz with special cut direction embedded at the end (near specimen) of transmitter bars; the shear strain is measured with a novel optical technique which is based on the luminous flux method. The feasibility of this methodology is demonstrated with the SHPSB experiments on a polymer bonded explosive (PBX). Square-shaped specimen is adopted. Experimental results show that the specimen is obviously rate-dependent. Shear and compression failure occur for the specimen.

### INTRODUCTION

The combined compressive and shear deformation at high strain rates ( $10^2$ - $10^4$  s<sup>-1</sup>) is encountered in several kinds of processing, such as grinding, machining, forming, events or processes that result in penetration. Stress wave studies, utilizing the uniaxial stress or strain condition, are commonly used to determine material response at high strain rates. Generally speaking, the mechanical response of materials subjected to complex stresses isn't consistent to the response at uniaxial condition. Studying the dynamic response of materials under combined compression-shear loading is important to get material behaviors more accurately and fully.

Koller[1] and Young[2] proposed two kinds of inclining impact test methods, where the fronts of longitudinal wave and shear wave weren't parallel. It's difficult to analyze the stress state quantitatively in these cases. Thirty years ago, Clifton and Abou-Sayed[3] designed an oblique-plate impact experiment based on gas gun, which was used to study constitutive models of materials at high pressures and strain rates ( $>10^4$  s<sup>-1</sup>). Compression-shear loading is attained by inclining the flyer, specimen and target plates with respect to the axis of the projectile in the same angle. Later on, many other scientists and engineers[4-11] continuously improved this technique. Pressure-shear experiments offer a unique capability for the characterizing materials under dynamic loading conditions. These experiments allow high pressures, high strain rates ( $10^4$ - $10^7$  s<sup>-1</sup>) and finite deformations to be generated. Pressure-shear plate impact testing, however, is limited to fine-grained materials, because the grain size must be small enough compared to specimen thickness to ensure that a representative average polycrystalline response is measured. Such experiments are lengthy because of the time required for specimen preparation. Huang and Feng[12] modified the torsional Kolsky (or split-Hopkinson) bar and designed the Kolsky-bar compression-shear

experiment which could be used to study the dynamic response of materials at high strain rates ( $10^2$ - $10^4$ ). This experimental method, however, doesn't really achieve combined compression-shear loading during loading. Because the speed of shear (or distortional wave) wave isn't equal to that of longitudinal wave. The specimen endures compression loading earlier, and it is subjected by shear loading when shear wave arriving. This situation is far from the actual condition. Meanwhile, for diminishing the stress and strain gradient from inner to outer of the wall, the tube specimens require a relative thin-wall thickness and a large diameter. For some materials, it's hard to satisfy.

This paper describes a newly developed combined compression-shear loading technique, the Split Hopkinson Pressure Shear Bar (SHPSB). The experimental setup, including the modified SHPB system, measurements for compression stress and strain, an optical system for the shear strain, and the quartz crystal for the shear stress measurements are discussed in EXPERIMENT. Experimental results of a PBX specimen are presented in RESULTS AND DISCUSSION, and conclusions are summarized finally.

## EXPERIMENT

The split Hopkinson pressure shear bar (SHPSB) technique is developed from the split Hopkinson pressure bar (SHPB). It is mainly consisted of a strike bar, an incident bar and two transmitter bars. The incident bar is same as the bar in SHPB at the close-to-projectile end, but the other end of the incident bar is wedge-shaped. The angle of the wedge is 90 degree as shown in Fig.1(a). The length and diameter of the incident bar is 1800 and 37mm, respectively. The length and diameter of the both transmission bars are 1000 and 20mm. In each experiment, there are two identical specimens respectively agglutinated between one side of the wedge and one of transmitter bars. When the strike bar impacts the incident bar, a loading impulse travels to specimens along the bar. Because of the special geometrical shape, interface of the specimen glued to the incident bar gets an axial and a transverse velocity. Thus, the specimens endure the combined compressive and shear loading at high strain rate.

There were three sets of strain gages located on the bars for compression-stress and strain measurements, and two quartz transducers with special cut direction ( $\Phi 20\text{mm} \times 0.25\text{mm}$ ) embedded at the end of transmission bars for shear stress measurement. A novel optical apparatus was employed to measure shear strain of specimen, which was based on the luminous flux method. The schematic of SHPSB is shown in Fig.1(b).

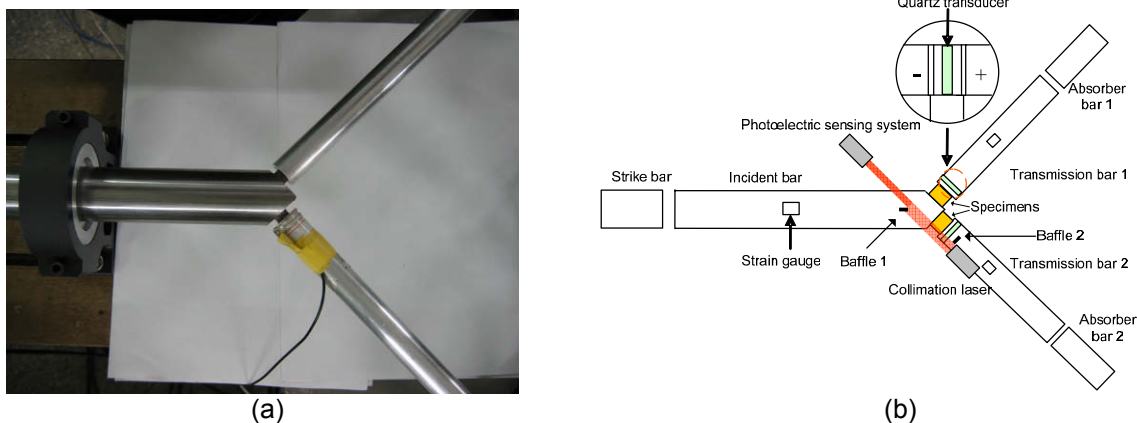


Fig. 1. (a) Photo of the experimental setups; (b) Schematic of the experiment apparatus

Following propagating stress wave theory, we know that there are two kinds of waves, a longitudinal wave and a bending (or flexural) wave in bars during the experiment. The transmission bars have an axial and a transverse motion, which correspond to longitudinal and bending wave. As the transmission bars are elastic, these two waves propagate independently. Because two transmission bars are symmetrical about the axis of the incident bar, no transverse movement is in existence. Similar with SHPB, the strike bar is great longer than the specimen in SHPSB experiments. So the specimens are under pressure and shear forces equilibrium during testing.

The compression stress in specimen can be deduced by axial strain from strain gauges mounted on the transmission bars. In fact, not only longitudinal wave arouses the axial strain in the transmission bars, but also bending wave results in the change of axial strain. When bending wave propagates in a thin bar, one part is in

compression, and the symmetrical part about the axis of the bar is in tension. In SHPSB experiment, a pair of strain gauges is mounted on each transmission bar at symmetrical locations. And these two strain gauges are settled at opposite arms in Wheatstone bridge. So the output voltage from bridge is a mean of the two strain gauges' voltage. Herein, the influence of bending wave to the axial strain of the bars is eliminated using the above method.

The compression stress of specimen is:

$$\sigma = \frac{A_t E \varepsilon_t}{A_s} \quad (1)$$

Where  $A_t$ ,  $A_s$  are respectively cross section areas of the transmission bars and incident bar;  $E$  and  $\varepsilon_t$  are respectively elastic module and the axial strain of the bar measured by the transmission strain gauges.

Based on the theory of stress wave[13], it's clear that longitudinal wave generates one dimension stress state in thin bar, and all shear stress terms are equal to zero. The shear stress in the transmission bar of SHPSB, therefore, is caused by bending wave, which is a kind of dispersion wave. Waves with different wavelength are of different phase velocities. As an important mechanics parameter in governing equation for bending wave, shear stress is frequently changing with wave propagation. It's hard to deduce the shear stress in specimen from the history of shear stress at some fixed locations on the transmission bar, similar to the operation in case of longitudinal wave. Thus, it requires that the shear stress gauge is closer to the specimen. In SHPSB experiments, we make use of quartz with special cut direction as shear stress gauge, which is just in response to shear stress. The distance between the quartz and the specimen is 2mm. If we neglect the tiny difference between the shear force in specimen and that of the transmission bar where quartz transducers embedded, the shear stress in specimen can be expressed with:

$$\tau = \frac{A_t \tau_t}{A_s} \quad (2)$$

Where  $\tau_t$  is the shear stress measured by the quartz transducer.

LS-DYNA is employed to simulate the SHPSB experiment. Numerical model is the same as the actual setup. To simplify the question, an elastic material model is chosen for the specimen. We validate the method of compression and shear stress measurement using the numerical results as shown in Fig.2.

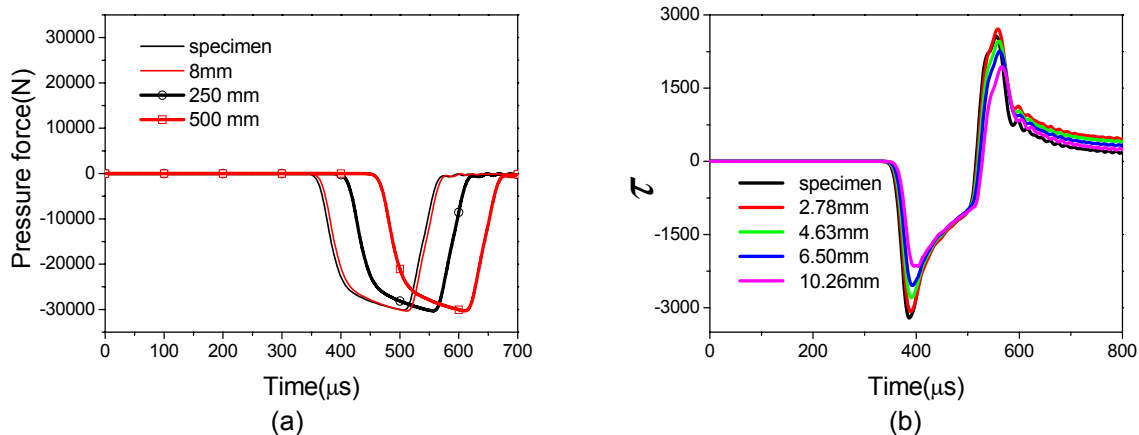


Fig. 2 (a) Average pressure force in the specimen and transmitted bar; (b) Average shear force in the specimen and transmitted bar

The “specimen” curve represents the average pressure force history of specimen in Fig.2(a), and the curve “8mm” stands for the average pressure force of two elements in the transmission bar, which is symmetric about the bar's axis. And these two elements are 8mm away from the specimen. So do the curves “250mm” and “500mm”. We can find that all curves are identical with each other in Fig.2(a), and it indicates that the method for measurement

of the compression stress is valid. Fig.2(b) shows the shear force histories at different position. The “specimen” curve is average shear force history of the specimen. And other curves represent the average shear force histories at different cross sections of the transmitted bars, which are respectively 2.78, 4.63, 6.50 and 10.26mm away from the specimen. In the range of 2.78mm, the shear force histories are identical with that of specimen. The relative peak difference between the shear force of specimen and that of the cross section which is in 2.78mm away from specimen is less than 5%. It implies that equation (2) is reasonable.

The sketch map of velocity analysis for the specimen of SHPSB is provided in Fig.3. The particle velocity at the incident bar end  $v$  can be divided into the axial velocity  $v_{1p}$  and transverse velocity  $v_{1\tau}$ , similarly, there are axial velocity  $v_{2p}$  and transverse velocity  $v_{2\tau}$  at the transmitter bar end. Thus, the compression and shear strain rates of the specimen are respectively:

$$\dot{\epsilon} = \frac{v_{1p} - v_{2p}}{l} \quad (3)$$

$$\dot{\gamma} = \frac{v_{1\tau} - v_{2\tau}}{l} \quad (4)$$

Where  $l$  is thickness of the specimen. Thus if we know the history  $v_{1p}$ ,  $v_{2p}$ ,  $v_{1\tau}$  and  $v_{2\tau}$ , we can calculate the compression and shear strain rates of the specimen using equation (3), (4). Furthermore, the compression and shear strain can be got by an integral operation.

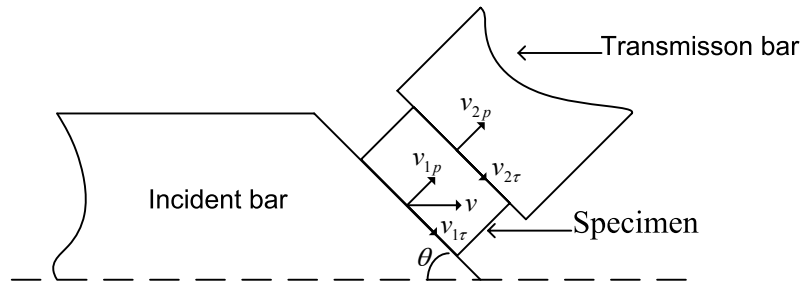


Fig. 3 Sketch map of velocity analysis for the specimen of SHPSB

For  $v_{1p}$  and  $v$ , there is relationship:

$$v_{1p} = v \sin \theta \quad (5)$$

Where  $\theta = 45^\circ$  is equal to the angle between axial direction of the incident bar and the transmission bar.

For one-dimensional elastic longitudinal wave, there is equation:

$$v = c_0 (\epsilon_i + \epsilon_r) \quad (6)$$

Because the elastic bending and longitudinal wave propagate independently in the transmission bar, thus

$$v_{2p} = c_0 \epsilon_t \quad (7)$$

Where  $c_0$ ,  $\epsilon_i$ ,  $\epsilon_r$  and  $\epsilon_t$  are respectively the velocity of longitudinal wave in the elastic bar, the incident strain and reflection strain measured by strain gauge mounted on the incident bar, and the transmission strain measured by the transmission strain gauge.

Substituting equation (5), (6), (7) into equation (3) yields

$$\dot{\epsilon} = \frac{c_0}{l} \left[ \frac{\sqrt{2}}{2} (\epsilon_i + \epsilon_r) - \epsilon_t \right] \quad (8)$$

And the compression strain of the specimen is:

$$\varepsilon = \int_0^t \frac{c_0}{l} \left[ \frac{\sqrt{2}}{2} (\varepsilon_i + \varepsilon_r) - \varepsilon_t \right] dt \quad (9)$$

For  $v_{1\tau}$  and  $v$ , there is also relationship:

$$v_{1\tau} = v \cos \theta \quad (10)$$

But, it's hard to know  $v_{2\tau}$  in experiments. So, we tried to get a difference of the transverse velocities or displacements at interfaces between the specimen and bars.

Ramesh and Narasimhan[14] proposed a method, known as the Laser Occlusive Radius Detector (LORD) to determine the radial deformations of specimens in SHPB experiments. Adding a collimated line head in front of the laser, Li[15] modified the LORD to measure the visco-plastic tensile strains in the SHTB (the split Hopkinson tension bar) experiments. We used a similar optical apparatus with Li to measure shear strain of the specimen. The optical setup for shear strain consists of three major components: an optical arrangement for generating a laser rectangular beam with uniform intensity per unit length, photoelectric sensing apparatus for detecting and measuring the light, the optical baffles fixed on the incident bar and transmission bar.

The optical emission system includes: a collimation laser operates at 660 nm with a 20 mW output power, which exports a collimated light beam with uniform intensity; an optical slit changes the circular light spot into the rectangular.

The photoelectric sensing part consists of a collecting lens and a photodiode light detector. The collecting lens focuses the incoming laser light into the photodiode detector, which is placed near its focus. The photodiode detector output is pre-amplified, and the optoelectronics and the preamplifier together are of 2 MHz bandwidth. The output voltage of the detector is proportional to total amount of the laser light collected. The whole system is at noise level less than 0.4 mV.

The optical baffles are respectively integrated firmly with bars by aluminum hoops. The relative displacement between optical baffles1 (on the incident bar) and optical baffles2 (on the transmission bar) is identical with that of two interfaces between the specimen and bars.

The basic ideal for measuring shear strain is very simple. The apparatus is mounted so that the light beam runs parallel with the axis of the transmission bar as shown in Fig.4(a). If the specimen and transmission bar just move along their axial direction, the width of laser beam will not change, and no signal outputs. If there is a few of relative transverse displacements of the two interfaces of the specimen with bars, optical baffles will block part of laser beam, and the changes of voltage will be recorded by oscilloscope. In other words, the optical apparatus is not sensitive to axial movement of the specimen, but very sensitive to transverse movement. Knowing the relationship of the width-change of laser beam and output voltage, we can get the transverse relative velocity ( $v_{1\tau} - v_{2\tau}$ ) or the transverse relative displacement.

To calibrate the optical system, we use a high precision gauge to partly block the laser beam, which is perpendicular to direction of the beam as shown in Fig.4(a). The blocking width ranges from 0 to 10 mm at a step of 0.1 mm. A specific blocking width ( $d$ ) corresponds to a light-blocking width  $\Delta d$  and a certain amount of voltage reading ( $\Delta U$ ) in the detector output. Fig.4(b) shows the results in two calibrating experiments, in which the locations of the high precision gauge is 4 centimeters apart. The  $\Delta d - \Delta U$  curve exhibits a good linearity, indicating a high uniformity of the laser sheet:

$$\Delta d = k \Delta U \quad (11)$$

where  $k=1.79$  mm/V is a calibration parameter of the optical system for the shear strain. So the shear strain is expressed with:

$$\gamma = \frac{\Delta d}{l} = \frac{k \Delta U}{l} \quad (12)$$

By differential operation, we can get the shear strain rates.

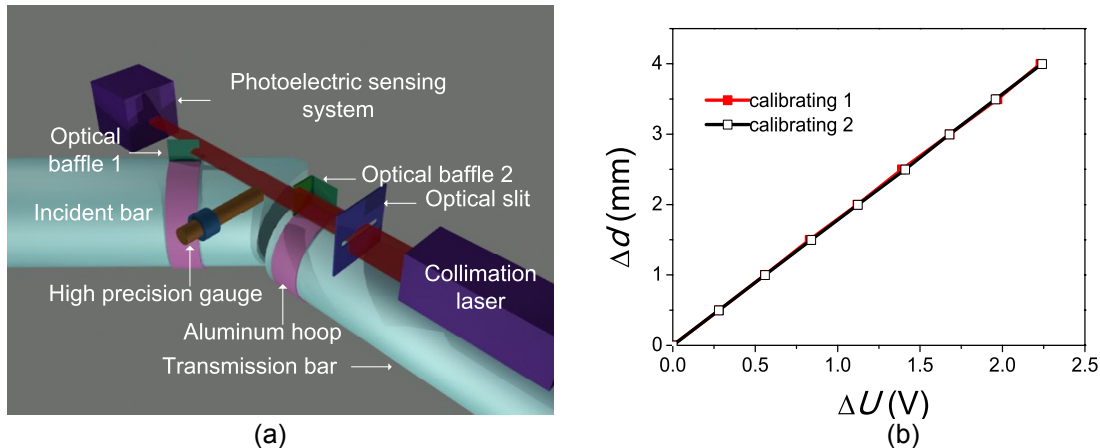


Fig.4(a) Schematic of calibration for the optical apparatus; (b) Results of the calibration experiments

## RESULTS AND DISCUSSION

To demonstrate the feasibility of the above technique, we have performed SHPSB tests on a polymer bonded explosives (PBX). The cubic specimens are made by molding. Size of the specimen is  $13\text{mm} \times 13\text{mm} \times 5\text{mm}$  as shown in Fig.5(a), with mass density of  $1.6\text{g}/\text{cm}^3$ . Fig.5(b) shows typical oscilloscope signals in the experiment. CH1 is connected to the strain gauge on the incident bar, recording the incident and the reflection longitudinal waves, CH2 is connected to the strain gauge on the transmission bar 2, recording the transmission longitudinal waves, CH3 is connected to the quartz crystal, measuring the shear force, and CH4 is connected to the optical system, monitoring the transverse motion of the specimen. The compression stress and strain of specimens are calculated by equation (1) and (9), and the shear stress and strain are calculated by equation (2) and (12).

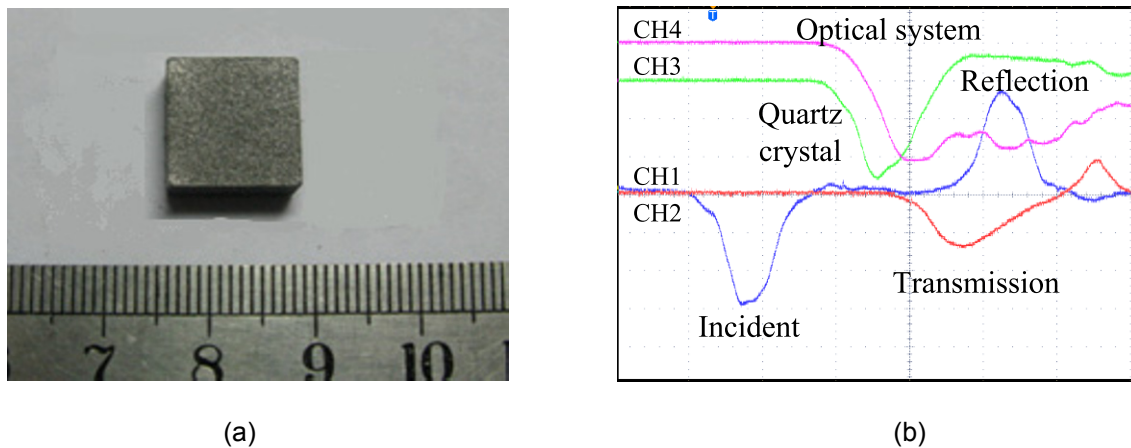


Fig.5 (a) Photo of the specimen; (b) Oscilloscope signals of test

Typical compression stress-strain curves obtained at high strain rates are shown in Fig.6(a). Average pressure strain rates at three levels are  $500$ ,  $540$  and  $600\text{s}^{-1}$ . And corresponding shear stress-strain curves are shown at various strain rates in Fig.6(b), and the average shear strain rates are  $450$ ,  $820$ ,  $750\text{s}^{-1}$ . In addition, the curves with the same symbol belong to one experiment in Fig.6.

From the Fig.6, we know that this PBX is sensitive to pressure strain rates, also to shear strain rates. At compression strain rates  $500\text{s}^{-1}$ , the peak compression stress is about  $12\text{MPa}$ , and the largest shear stress is about  $1.8\text{MPa}$  in this experiment. In fact, these two peak values are not corresponding to each other. As shown in Fig.7(a) for a typical test, we calculate the compression stress and shear stress histories. The time corresponding to the peak of shear stress curve is earlier than the time corresponding to the peak of compression stress curve. The compression strain and shear strain histories are shown in Fig.7(b). The vertical lines in Fig.7 represent the times when the compression and shear stresses getting to the peak. Before the compression and shear strains

arriving at the peak value, the shear and compression stresses reach the largest values. In other words, after reaching the peak value, the shear stress begins to drop with the strain sequentially increasing. It indicates that two kinds of failure modes (shear and compression failure) occur for the specimen, and shear failure occurs before compression failure appearing. It's identical with the fact that the shear strength is less than compression strength for this kind of material.

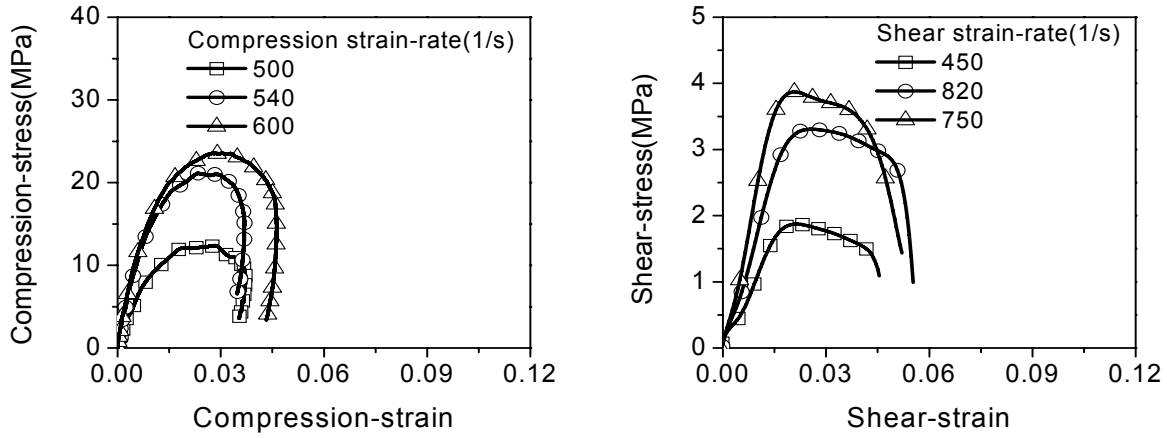


Fig. 6 (a) Engineering compression stress-strain curves; (b) Engineering shear stress-strain curves;

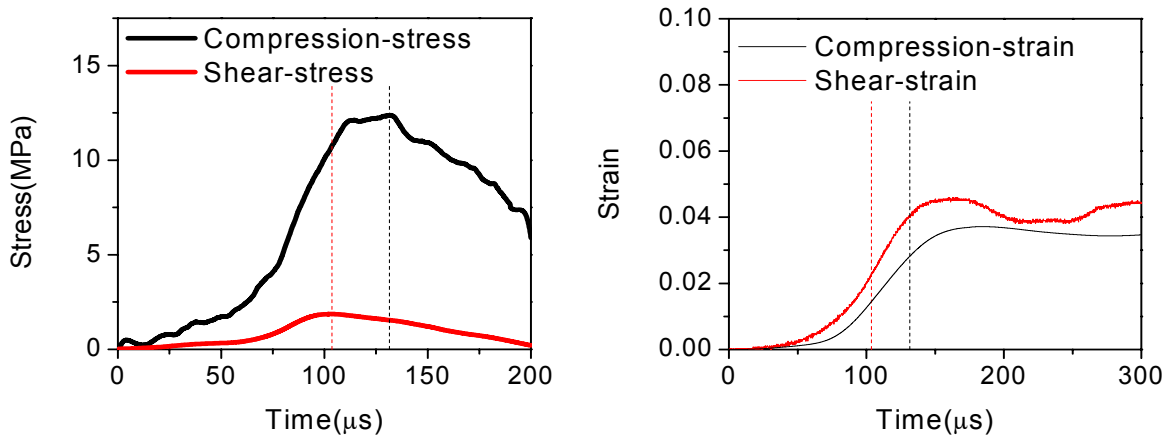


Fig. 7 (a) Compression and shear stress histories curves; (b) Compression and shear strain histories curves;

## CONCLUSION

We propose a modified SHPB testing method, SHPSB technique, to measure the dynamic responses of specimens under combined compression-shear loading at high strain rates ( $10^2$ - $10^4$ ). In this method, strain gauges are employed to measure the compression stress and strain of specimens, piezoelectric force transducers are embedded in the transmitted bars in order to measure the loading shear force, and an optical apparatus based on the luminous flux method, is used to monitor the transverse motion of specimens, from which the average shear strain is deduced. The feasibility of this technique is demonstrated with the SHPSB experiments on a PBX. The experimental results show that this PBX is sensitive to strain rates, and shear and compression failure occur for the specimen, and shear failure occurs before compression failure appearing. This technique is readily implementable and can be applied to investigating dynamic-mechanics property of materials under complex stress state.

## ACKNOWLEDGMENTS

This work was supported by the Natural Science Foundation of China (NSFC) through Grant No. 10672177 & 10872215 and 10902100. And we would like to acknowledge the support of National Key Laboratory Foundation under grant NO.9140C670902090 and Science Foundation of CAEP under grant NO.2009A0201008.

**REFERENCES**

- [1] Koller L. and Fowles G., "Compression-shear waves in Arkansas novaculite", In: Timmerhaus K. Barber M., eds. High Pressure Science and Technology, Proceedings of Sixth AIRAPT Conference, Boulder CO, 1977. New York: Plenum Press, 2: 927 (1979).
- [2] Young C. and Dubugnon O., "A reflected shear-wave technique for determining dynamic rock strength", *Int J Rock Mech Min Sci & Geomech Abstr.* 14: 247-259 (1977).
- [3] Abou-Sayed A.S., Clifton R.J., and Hermann L., "The oblique-plate impact experiment", *Exper Mech.* 127-132 (1976).
- [4] Gilat A. and Clifton R.J., "Pressure-shear waves in 6061-T6 aluminum and alpha-titanium", *J Mech Phys Solids.* 33: 263-284 (1985).
- [5] Prakash V. and Clifton R.J., "Time resolved dynamic friction measurements in pressure-shear". in: Vol. 165 *Experimental Techniques in the Dynamics of Deformable Bodies.* 33-47 (1993).
- [6] Machcha A.R. and Nemat-Nasser S., "Effects of geometry in pressure-shear and normal plate impact recovery experiments: Three-dimensional finite-element simulation and experimental observation", *J Appl Phys.* 80: 3267-3274 (1996).
- [7] Tong W., "Pressure-shear stress wave analysis in plate impact experiments", *int.J.Impact enging.* 19: 147-164 (1997).
- [8] Frutschy K.J. and Clifton R.J., "High-temperature pressure-shear plate impact experiments using pure tungsten carbide impactors", *Exper Mech.* 38: 116-125 (1998).
- [9] Frutschy K.J. and Clifton R.J., "High-temperature pressure-shear plate impact experiments on OFHC copper", *J Mech Phys Solids.* 46: 1721-1743 (1998).
- [10] Prakash V., "Time-resolved friction with applications to high-speed machining: Experimental observations", *Tribology Transactions.* 41(2): 189-198 (1998).
- [11] Page N.W., Yao M., Keys S., et al., "A high-pressure shear cell for friction and abrasion measurements", *Wear.* 241: 186-192 (2000).
- [12] Huang H. and Feng R., "A study of the dynamic tribological response of closed fracture surface pairs by Kolsky-bar compression-shear experiment", *International Journal of Solids and Structures.* 41(11-12): 2821-2835 (2004).
- [13] Graff K., *Wave motion inelastic solids*, Columbus: Ohio University Press, (1975).
- [14] Ramesh K.T. and Narasimhan S., "Finite deformations and the dynamic measurement of radial strains in compression Kolsky bar experiments", *International Journal of Solids and Structures.* 33(25): 3723-3738 (1996).
- [15] Li Y. and Ramesh K.T., "An optical technique for measurement of material properties in the tension Kolsky bar", *International Journal of Impact Engineering.* 34: 784-798 (2007).